

Time-Transformations for Reversible Variable Stepsize Integration

Stephen D. Bond and Benedict J. Leimkuhler *

*Department of Mathematics
University of Kansas
Lawrence, KS 66045*

The development of a Sundman-type time-transformation for reversible variable stepsize integration of few-body problems is discussed. While a time-transformation based on minimum particle separation is suitable if the collisions only occur pairwise and isolated in time, the control of stepsize is typically much more difficult for a three-body close approach. Nonetheless, we find that a suitable choice of time-transformation based on particle separation can work quite well for certain types of three-body simulations, particularly those involving very steep repulsive walls. We confirm these observations using numerical examples from Lennard-Jones scattering.

Keywords: Adaptive Verlet method, time-reversible methods, adaptive timestepping, variable stepsize methods, N-body mechanical problems, scattering, Verlet

AMS Subject classification: 70-08, 70F05, 70F07, 70F10, 70H05

1. Introduction

For a conservative (i.e. Hamiltonian) system, the natural integration paradigm is the symplectic map, a subject of much recent interest. For such maps, it is possible to show the existence of a perturbed Hamiltonian function¹ whose exact dynamics replicate the numerical solution, up to an error term exponentially small in the timestep ($O(e^{-1/\Delta t})$), for a long (but finite) interval in time [1–3]. The presence of this approximate conserved quantity appears to confer greater numerical stability on the numerical simulation. In practice, when integrating a system with smooth dynamics using a symplectic integrator with sufficiently small stepsize, one observes that the energy of the numerical solution oscillates chaotically, but with little discernible secular growth or decay, even during very long time integrations.

The situation may be quite different, however, when the system is subject to very strong localized forces, e.g. when integrating collisional N-body dynamics involving a Coulombic or hard soft-wall (inverse power law) interbody potential. Here we observe that energy error varies rapidly at the impacts of the bodies, and may even jump to a new energy level during a collision. While a sufficiently small timestep will typically force the simulation into the regime where the asymptotic treatment can be applied, this timestep restriction may be unrealistic for practical purposes, particularly away from the points of collision. For this reason, it is natural to attempt to incorporate some sort of variable stepsize strategy to improve the behavior of the simulation.

*The authors were supported by NSF Grant No. DMS-9627330.

¹The perturbed Hamiltonian is developed as a series expansion with the terms of this expansion obtained by matching the associated perturbative dynamics with the asymptotic expansion of the numerical solution.

Unfortunately, as shown by Sanz-Serna and Calvo [4], a symplectic method does not perform as well when the stepsize is varied as when the stepsize is held fixed. There are at least two reasonable explanations for this. First, one may observe that the stepsize is typically being computed from an error estimate. In this sense, the stepsize is itself a function of the phase variables. The dependency of one step on the previous step must therefore include the functional dependence of the stepsize on that previous step. The combined mapping is therefore typically not symplectic even when it is based on a symplectic fixed stepsize integrator. An alternative explanation is that the perturbative series expansion for the “nearby Hamiltonian” of a symplectic integrator is only generally meaningful when the numerical solution can be viewed as the iteration of a single symplectic one-step method.

Despite this rather pessimistic state of affairs, it turns out that a symplectic treatment with variable stepsizes is possible. The idea is to introduce a *Poincaré transformation* [5,6] of the Hamiltonian $H = H(q, p)$:

$$\tilde{H} = g(q, p)(H - H_0), \quad g > 0,$$

where g is a “control” or “monitor function”. Along the energy slice $H = H_0$, the dynamics of the transformed system will be equivalent to those of the original system, up to a transformation of time. To see this, write the Hamilton’s equations

$$\begin{aligned} \dot{q} &= g \nabla_p H + (H - H_0) \nabla_p g, \\ \dot{p} &= -g \nabla_q H - (H - H_0) \nabla_q g, \end{aligned}$$

then observe that when $H = H_0$, the equations are the same

as the original equations expressed in a new time variable, say τ , satisfying

$$\frac{dt}{d\tau} = g(q, p). \quad (1)$$

A major disadvantage of the general Poincaré transformation is that it mixes the variables so that an explicit symplectic treatment of the extended Hamiltonian is no longer possible, and we are compelled to use implicit symplectic methods (see [3,7]). A first order method can however be made semi-explicit in the case of an N -body system with separated Hamiltonian function $T(p) + V(q)$, but a second order method is often required for accuracy reasons. A more serious defect associated with the Poincaré transformation is that it allows the numerical solution to leave the energy slice $H = H_0$, effectively destroying the precise relationship (through (1)) between t and τ .

In this article we consider Hamiltonian systems with time-reversal symmetry (i.e. $H(q, -p) = H(q, p)$). For such problems there is a less expensive alternative approach which appears to yield—at least to some extent—the benefits of a symplectic method, even though it is not in fact symplectic. The idea is to replace the Poincaré transformation by direct use of the Sundman transformation (1) and then to solve the ODEs

$$\dot{q} = g \nabla_p H, \quad (2)$$

$$\dot{p} = -g \nabla_q H. \quad (3)$$

This new system is rarely a Hamiltonian system (this would only be the case if $g = \tilde{g}(H(q, p))$ for some scalar function \tilde{g}). Nonetheless, if $g(q, -p) = g(q, p)$ and $g(q, p) > 0$, then the new system will retain the time-reversal symmetry present in the original system. As we outline in the next section, an explicit time-reversible integrator is available for the reparameterized system, namely the Adaptive Verlet method proposed by W. Huang and the second author [8].

Like symplecticness, the time-reversal symmetry is a strong geometric property of the flow of a mechanical system. Over long time simulations, methods which preserve the time-reversal symmetry can exhibit improved stability [9–11] when compared to standard integration methods. Unlike symplecticness, time-reversal symmetry of a numerical integration scheme does not in general confer an approximate integral obtainable through an asymptotic expansion. One case where such a result is available is in the case of the two-body problem, where it follows readily from the strong symmetry of the system [10]. For Coulombic few-body problems, time-reversible schemes can also be applied in concert with Kustaanheimo-Stiefel transformations [10] and appear to demonstrate excellent long-term preservation properties.

Energy conserving schemes have been considered by several authors [12–15]. These methods can preserve energy

and/or angular momentum, as well as reversing symmetry, but not simultaneously energy and symplectic structure, due to a celebrated result of Ge and Marsden [16]. While reversible energy-momentum methods have occasionally proven effective, these methods are necessarily implicit; the need to solve a system of nonlinear equations at each timestep typically limits the effectiveness of the methods.

A key barrier to the wider use of the reversible adaptive methods is the design of appropriate time-transformation functions g . For the two-body problem, it is usually possible to develop a time-transformation based on minimum particle separation, but it is not clear that such an approach would adequately adjust the timestep in the vicinity of a three-body close approach. In this article, we explore the application of the reversible approach with special attention to the problem of a few particles interacting under a Lennard-Jones type potential.

2. Adaptive Verlet

The equations (2)-(3) are discretized by a special second order scheme, as first proposed in [8]:

$$q^{n+1/2} = q^n + \Delta t_n \nabla_p H(q^n, p^{n+1/2}), \quad (4)$$

$$p^{n+1/2} = p^n - \Delta t_n \nabla_q H(q^n, p^{n+1/2}), \quad (5)$$

$$\frac{2\mathcal{R}}{\Delta s} = \frac{1}{\Delta t_{n+1}} + \frac{1}{\Delta t_n}, \quad (6)$$

$$q^{n+1} = q^{n+1/2} + \Delta t_{n+1} \nabla_p H(q^{n+1}, p^{n+1/2}), \quad (7)$$

$$p^{n+1} = p^{n+1/2} - \Delta t_{n+1} \nabla_q H(q^{n+1}, p^{n+1/2}), \quad (8)$$

where \mathcal{R} is one of the following expressions:

$$\mathcal{R}_1 = 2g(q^{n+1/2}, p^{n+1/2}),$$

$$\mathcal{R}_2 = g(q^{n+1/2}, p^n) + g(q^{n+1/2}, p^{n+1}),$$

$$\mathcal{R}_3 = g(q^n, p^n) + g(q^{n+1}, p^{n+1}).$$

Note that the first choice leads to an explicit method in the case of a separable Hamiltonian (i.e. $H(q, p) = T(p) + V(q)$); the second is semi-explicit and the last is fully implicit. For the numerical experiments in this article, we will use the explicit method, \mathcal{R}_1 . For details and differences between the methods, the reader is referred to [8,17]. The reason for using the reciprocal of the timestep in (6) is not immediately obvious, but this approach was found to behave well in numerical experiments. Very recently, a precise rationale for this choice has been given based on an asymptotic (“backward error”) analysis of the resulting method [18].

3. Power Law Potentials and The Time Reparameterization Function

We now consider a simple model problem for the hard soft-wall, the one degree of freedom problem with Hamilto-

nian

$$H = \frac{p^2}{2} + q^{-\alpha}.$$

In this system α is a fixed parameter, which determines the strength of the repulsive wall. For a given set of initial conditions, q may become rather small, resulting in a large time-localized force. We would like to introduce a rescaling of time, which decreases the severity of this problem. We therefore introduce a Sundman transformation of the form

$$g_1(q, p) = q^\beta,$$

leading to the following equations of motion:

$$\begin{aligned} \frac{dq}{d\tau} &= q^\beta p, \\ \frac{dp}{d\tau} &= \alpha q^{\beta-\alpha-1}. \end{aligned}$$

What value of β gives optimal control of the simulation?

In some sense, we would like β to be as small as possible, since a larger β will add to the number of timesteps, and hence the work, performed during the collision event. We choose the value of β using a simple technique.

3.1. Optimal selection of β for hard soft-wall potentials

Consider an orbit of the (untransformed) one-degree of freedom system. The particle starts from a distant point with momentum $p_{-\infty}$, approaches the point of collision $q = q_{\min}$. During a short time interval, the momentum changes sign and the particle position tends to infinity with asymptotic value $p_{+\infty} = -p_{-\infty}$. The situation is illustrated in Figure 1. Assuming that the wall is rather steep, we can calculate, approximately, the duration of the collision as follows.

Assume an energy $E > 0$. Far from the wall, the energy is all kinetic, so we have

$$|p_{\pm\infty}| = \sqrt{2E}.$$

Note that, for a hard soft-wall, this is also the value of the momentum until just prior to the time of collision, when it changes very suddenly. At the point of collision, on the other hand, $p = 0$ and $q = q_{\min}$, implying that

$$q_{\min}^{-\alpha} = E.$$

This allows us to solve for $p_{\pm\infty}$ in terms of q_{\min} :

$$|p_{\pm\infty}| = \sqrt{2E}^{1/2} = \sqrt{2}q_{\min}^{-\alpha/2}. \quad (9)$$

Near the point of close approach, the positional motion slows, almost to a stop, while the momentum changes sign very suddenly according to the differential equation

$$\dot{p} \approx \alpha q_{\min}^{-\alpha-1},$$

thus, with T the total time for this collision,

$$p_{+\infty} - p_{-\infty} \approx \alpha q_{\min}^{-\alpha-1} T.$$

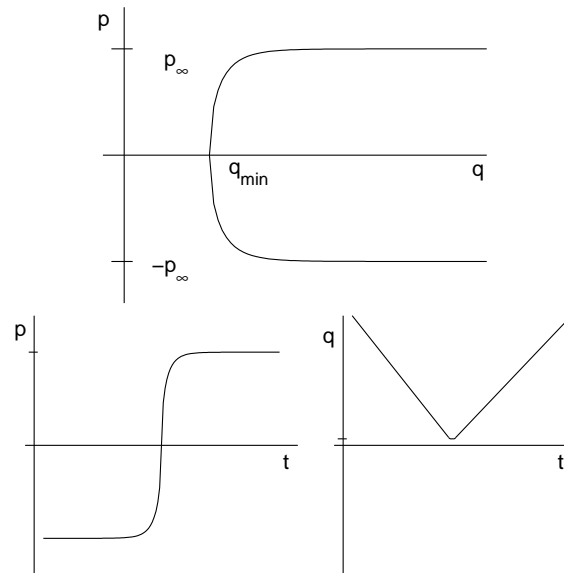


Figure 1. A collision test orbit in a single degree of freedom model with a hard soft-wall. A typical orbit in phase space is shown in the upper panel. In the lower panel, the corresponding evolution of q and p are plotted with respect to time.

But since $p_{-\infty} = -p_{+\infty}$ and using (9), we have

$$2\sqrt{2}q_{\min}^{-\alpha/2} \approx \alpha q_{\min}^{-\alpha-1} T,$$

or

$$T \approx \frac{2\sqrt{2}}{\alpha} q_{\min}^{\alpha/2+1}.$$

To put this into words, the stronger and sharper the wall, the shorter the duration of the collision.

Now let's repeat this exercise in the case of rescaling with $g(q) = q^\beta$, that is, let's determine the total fictive time during which the collision takes place. Using the same basic procedure and the fact that the relationship (9) is undisturbed by the scaling (energy is still a conserved quantity), we find that the collision now lasts τ units of fictive time, where

$$\tau \approx \frac{2\sqrt{2}}{\alpha} q_{\min}^{-\beta+\alpha/2+1}. \quad (10)$$

Based on this formula, we propose the choice $\beta = \frac{\alpha+2}{2}$ as approximately optimal. With this value, we make the fictive time collision duration uniform with respect to q_{\min} . In other words, no matter the energy level, by using $\beta = \frac{\alpha+2}{2}$, the collision event will require approximately the same amount of fictive time, so that sharper collisions (which would normally happen very rapidly) are “slowed down” in the rescaled time so that they evolve on the same time scale as relatively weak collisions. The choice of β can therefore be viewed as rendering the resulting equations *scaling invariant* in a certain sense. For a survey and related discussion, see [19].

We expect this estimate of optimal β to be valid for the *high energy* regime, i.e., when q_{\min} is rather less than unity, so that the exponential part of (10) is most critical. It should be pointed out that, with fixed energy E , we know that $q_{\min} = E^{-1/\alpha} \rightarrow 1$ with increasing α . The optimal choice of β therefore becomes less critical for large values of α at low energy.

3.2. Stepsize Bounds

An important observation is that the choice of time-transformation motivated by control of the error near collision may lead to instabilities during the “smooth regime.” We can draw an interesting parallel here with work on stiff differential equations: it is important that a variable stepsize technique introduced for controlling step during rapid transients not lead to inefficiencies away from the transient, i.e. during the “stiff phase.”

Intuitively, we would like the asymptotic behavior of our system to remain unchanged under time transformation. To investigate the situation, we start by writing the system as a second-order differential equation:

$$\frac{d^2q}{d\tau^2} = \frac{\beta}{q} \left(\frac{dq}{d\tau} \right)^2 + \alpha q^{2\beta-\alpha-1}.$$

For the untransformed system, one can clearly see that the acceleration goes to zero as q goes to infinity, so that asymptotically q moves along a straight line. This is not the situation in the rescaled dynamics if $2\beta \geq \alpha + 1$. In this case the acceleration will increase monotonically, and we will not have linear motion as q goes to infinity; indeed, q may tend to infinity in a finite number of steps.

This strong (and unfortunate) restriction in the choice of β can be eliminated by using a modified transformation function g of the form

$$g_2(q) = (c + q^{-\beta})^{-1}, \quad c > 0.$$

If the constant c is small, we have simply introduced an asymptotic upper bound on the time rescaling. In our new time variable, τ , the equations of motion are

$$\begin{aligned} \frac{dq}{d\tau} &= (c + q^{-\beta})^{-1} p, \\ \frac{dp}{d\tau} &= \alpha (c + q^{-\beta})^{-1} q^{-\alpha-1}, \end{aligned}$$

or

$$\frac{d^2q}{d\tau^2} = \frac{\beta}{cq^\beta + q} \left(\frac{dq}{d\tau} \right)^2 + \alpha q^{-\alpha-1} \left(\frac{1}{c + q^{-\beta}} \right)^2$$

As $q(\tau)$ goes to infinity, the acceleration goes to zero. We conclude this section with a proposition summarizing our observations.

Proposition 1. For a hard soft-wall collision, the choice

$$g(q) = (c + q^{-\beta})^{-1}, \quad c > 0, \quad \beta = (\alpha + 2)/2.$$

combines (1) uniform fictive collision time (independent of energy level), and (2) straight-line motion as $q \rightarrow \infty$.

4. Numerical Experiments: The Lennard-Jones Potential

A common application for Power-Law potential functions arises in molecular modeling. Combinations of such potential functions are used to model the repulsive and attractive interactions between non-bonded atoms. One of the most commonly used potentials of this form is the Lennard-Jones potential,

$$V(q) = 4\epsilon \sum_{i>j} \left[\left(\frac{\sigma}{r_{ij}} \right)^{12} - \left(\frac{\sigma}{r_{ij}} \right)^6 \right]$$

In this model ϵ and σ are constants, and r_{ij} is the distance between the i th and j th atoms. $V(q)$ can change quite rapidly whenever one of these distances is small. In Figure 2, several level curves of the Hamiltonian are shown to illustrate the characteristics of a typical orbit. While low energy simulations lead to periodic trajectories, higher energy levels can cause an atom to be ejected from the system. One should also observe that when the distance between the atoms is at a minimum, the momenta changes rapidly, due to the strong forces. If the timestep is not small enough, these forces can lead to nonphysical jumps in the energy. On the other hand, if all of the atoms are far apart, the forces in the system are quite small. In this regime, there is no need for adaptive timestepping. The control function proposed in the previous section meets these criteria. While this control function

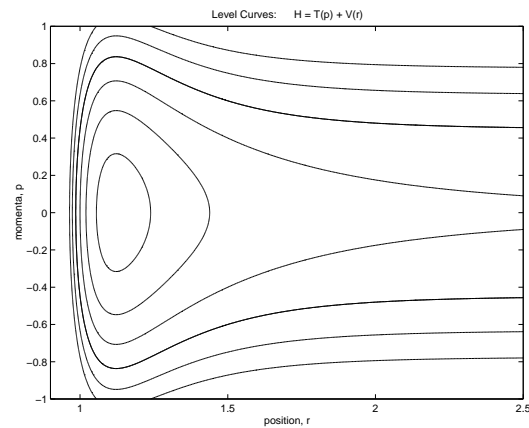


Figure 2. The 2-body Lennard-Jones problem. The level curves of the Hamiltonian are shown in phase space, indicating differences between high and low energy trajectories.

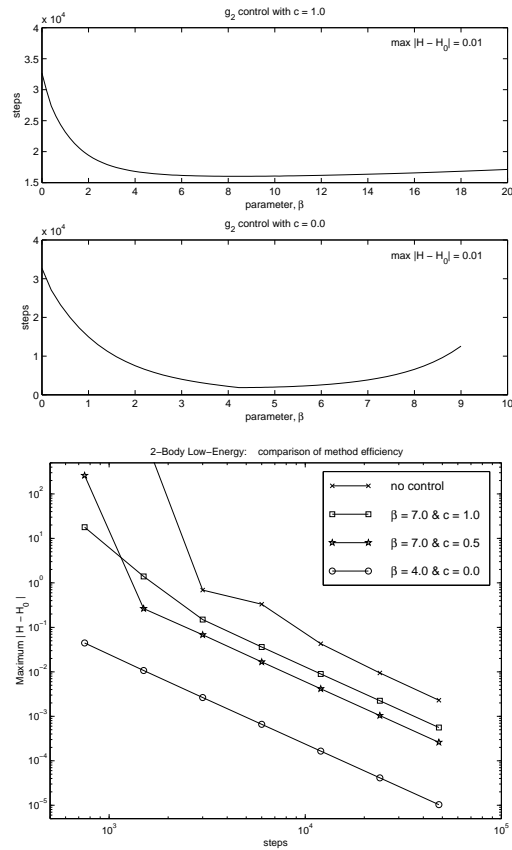


Figure 3. The optimal control parameter for the 2-body Lennard-Jones Problem. The work is plotted as a function of β for a fixed error level, in the upper and center panels. The lower panel shows the work error diagram, illustrating the benefits of control.

was designed for a one dimensional problem, we can easily extend it to an N-body system in the following way: ²

$$g_2(q) = \left(c + r_{\min}^\beta \right)^{-1} \quad \text{with} \quad r_{\min} = \min_{i,j} r_{ij}$$

4.1. Two-Body Problem

As a numerical experiment, we find the optimal β for the g_2 control function, as it is applied to the low energy two-body Lennard-Jones problem. Two atoms are started at an initial separation of 2.5 units, with no initial momenta. During the course of the simulation, they repeatedly collide, generating a periodic solution. The error in the simulation is gauged by maximum deviation in energy over the length of the run. In order to assess the efficiency of each choice of β , the stepsize is adjusted to hold the maximum energy deviation constant between runs.

²For the general N-body problem, the function $g_2(q)$ is continuous but not differentiable. While the method does not use derivatives of the control, it may be needed for backward error analysis. A smoothed version of this control can be obtained by substituting $\sum_{i,j} \left(r_{ij}^{-p} \right)^{-1/p}$ for r_{\min} , with p large.

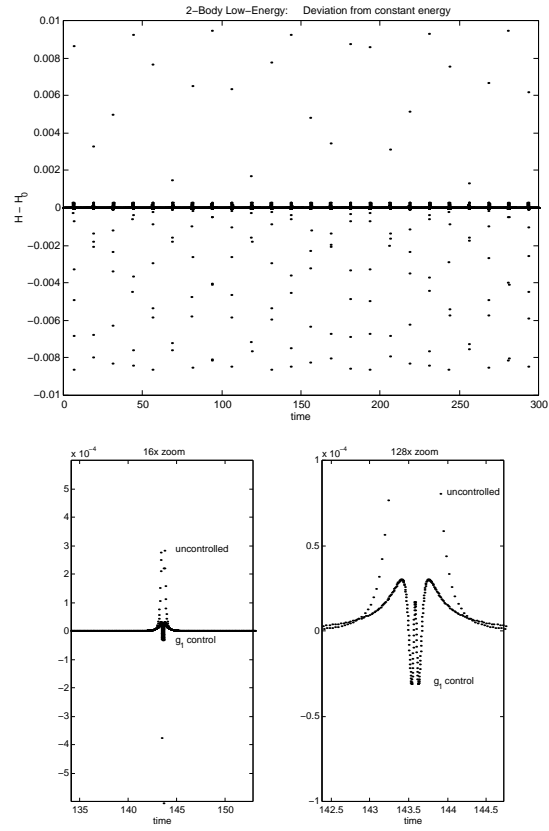


Figure 4. Improvements in conservation of energy for the 2-body Lennard-Jones problem. The conservation of energy for the fixed stepsize method and the adaptive method (control function g_1 with $\beta = 4$) is shown in the upper panel. Close-ups of the energy conservation over a single collision are given in the two lower panels, illustrating the concentration of steps taken in the vicinity of an impact.

In Figure 3, the work as a function of β is plotted for a fixed error level. From our analysis in the previous sections, we expect $\beta = 7$ to be optimal, if the repulsive part of the potential dominates the interactions. This will only be the case when the separation between the atoms is near a minimum. By increasing the value of c , we can increase the localization of our control. When the effect of the control is sufficiently localized ($c = 1.0$), we find that $\beta = 7.0$ is indeed nearly optimal. One should note that we get more of an optimal range for β , than a single optimal value, especially when $c > 0$.

On the other hand, if we set c to zero, the control has strong effects away from the collisions. For this case, we find that $\beta = 4.25$ is optimal, since the attractive force now influences our parameter choice. Figure 3 also shows the efficiency of the controlled and uncontrolled methods. In our particular test problem the trajectory remains bounded, eliminating the need for c . It is not surprising that we find the greatest improvements in the efficiency of the algorithm when c is set to zero.

In Figure 4 the deviation in energy using the most efficient g_2 control is compared with the uncontrolled method.

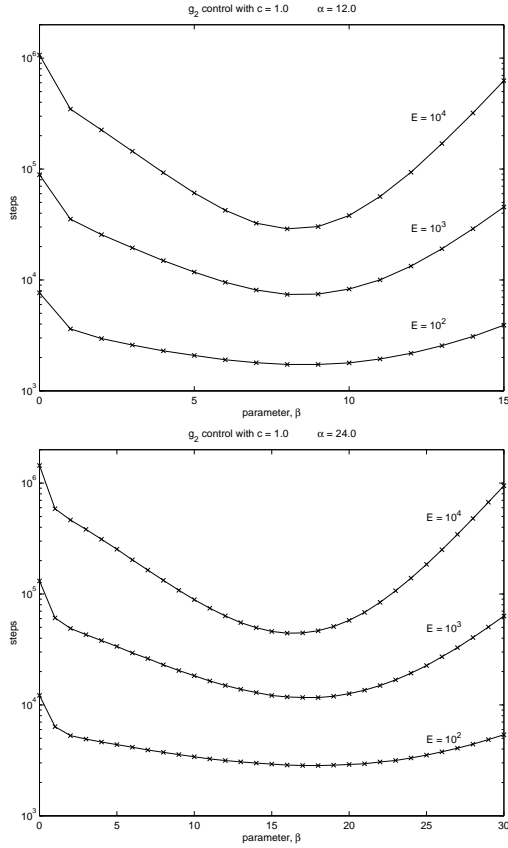


Figure 5. The optimal control parameter for the hard soft-wall problem. In the upper panel, the work is shown as a function of β for a fixed error level using $\alpha = 12.0$, and for various energy levels ($E = 10^2$, 10^3 , and 10^4). In the lower panel a similar figure is given for $\alpha = 24.0$.

This figure illustrates how the controlled method is able to dramatically improve the efficiency of the integration. It takes very small steps whenever the separation between the two atoms becomes small. This allows for a more accurate resolution of the dynamics in the vicinity of this “collision”. For this simple problem, we can achieve improvements of several orders of magnitude by introducing stepsize control.

As a final two-body numerical experiment, we return to the model problem for the hard soft-wall, with Hamiltonian

$$H = \frac{p^2}{2} + q^{-\alpha}.$$

We would like to understand how the adaptive method performs for different energy levels, and different values of α . We begin with the case of Lennard-Jones repulsion, i.e. $\alpha = 12.0$. We start our simulation with q large, and with the initial momenta negative. There is a single collision event, and then the particle is ejected. Our analysis in the previous section has indicated that for the g_2 control, $\beta = 7.0$ should be nearly optimal. However, this analysis was based on a simulation at high energy, and we would like to investigate how the optimal value of β varies with changes in energy. We hold the maximum deviation in the energy constant, and

vary the parameter β . In the upper panel, in Figure 5, the number of steps is shown as a function of β for three different energy levels. At low energy levels, the curve is rather flat, and we see more of a range of optimal values than a single optimal choice. As the energy level is increased, the minimum in the curve becomes more pronounced. We find that $\beta = 7.0$ is nearly optimal at the highest energy level. In the lower panel, in Figure 5, we show the same curves for $\alpha = 24.0$. Here we see a similar trend, with $\beta = 13.0$ nearly optimal in the more energetic simulations.

4.2. Three-Body Problem

The dynamics of the system are dramatically changed by the addition of a third body. Many of the symmetries present in the two-body problem are no longer preserved. During a many-body simulation, the amount of energy present in three-body interactions may be much higher than for two bodies. We would like to investigate possibility of strong three-body interactions (i.e. during triple “collisions”) and whether a control function based on three body interactions is required to efficiently resolve the dynamics.

We construct our three-body control functions as extensions of the two-body control g_2 . This is a natural construction since one would like these new functions to behave similar to g_2 during two-body “collisions”. Composing g_2 with the elementary symmetric functions [20] of order three, we get three new control functions:

$$\begin{aligned} g_3(q) &= \left((c + r_{12}^{-\beta}) (c + r_{13}^{-\beta}) (c + r_{23}^{-\beta}) \right)^{-1/3} \\ g_4(q) &= \left(\left((c + r_{12}^{-\beta}) (c + r_{23}^{-\beta}) \right)^{1/2} \right. \\ &\quad \left. + \left((c + r_{12}^{-\beta}) (c + r_{23}^{-\beta}) \right)^{1/2} \right. \\ &\quad \left. + \left((c + r_{12}^{-\beta}) (c + r_{13}^{-\beta}) \right)^{1/2} \right)^{-1} \\ g_5(q) &= \left((c + r_{12}^{-\beta}) + (c + r_{13}^{-\beta}) + (c + r_{23}^{-\beta}) \right)^{-1} \end{aligned}$$

In order to study the effects of these new control functions over a wide range of interactions, we consider the three-body scattering problem. We place two atoms close together, in a periodic trajectory, and fire a third atom into the system. The offset at which the third body is fired, is varied by specifying a scattering parameter, δ . We then record the angle, θ , at which this third body asymptotically exits the system. In Figure 6 we show the initial conditions, and the relationship between δ and θ . Rapid fluctuations in the scattering plot indicate a sensitive dependence of the solution on the initial conditions.

In our numerical experiment, the scattering parameter, δ , is chosen at 1000 evenly spaced points between -3 and 3 .

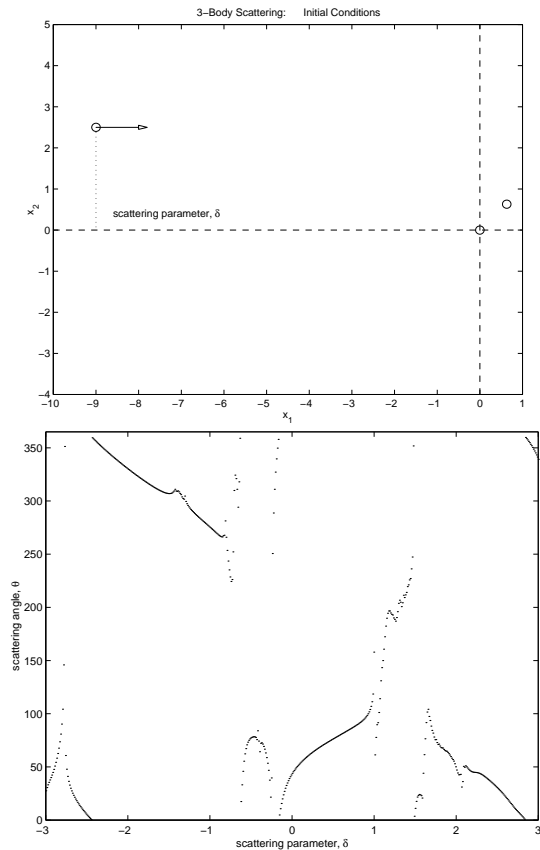


Figure 6. The 3-Body Lennard Jones Scattering Problem. The initial conditions, which depend on a scattering parameter, δ , are shown in the upper panel. The lower panel shows the exit (or scattering) angle of one particle, as a function of δ .

We allow each control function to prescribe an average of 2500 steps per run. This will make the total work over all the initial conditions equal for each variation of our method. For each run, we record the maximum energy error and the number of steps required by the method. The parameters c and β are set to 0.1 and 6.0, respectively. This pair of parameter values was found to be an optimal pair in our two-body simulations.

In Figure 7 the error and work are shown as functions of the scattering parameter. From the error diagram, one can see that g_2 is the most efficient control for this problem. This is an interesting result, since it is based purely on two-body interactions. While many of the initial conditions did lead to strong three-body interactions, these interactions were sufficiently resolved by g_2 . The work diagrams show the variation of the work required for each run. The control allows us to not only improve the efficiency in each run, but also over a large number of runs. The relatively constant error curves for the controlled method, indicate its reliability for this type of problem. One should also note that, when using the g_2 control, the largest errors are obtained for δ about 1.4 (which is also, incidentally, the parameter value for which the largest number of steps was prescribed by that control).

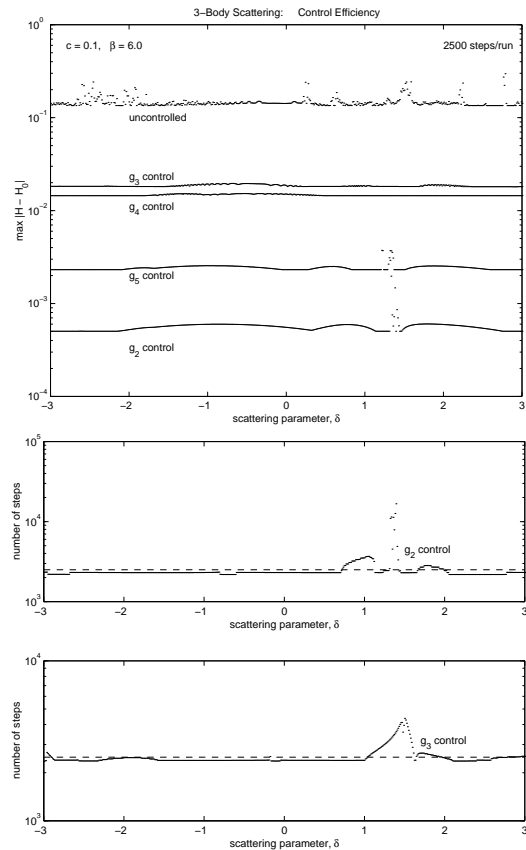


Figure 7. Efficiency of the methods when applied to a 3-body scattering problem, with the total work held constant. Each plot reflects a total of 1000 different simulations, over a wide range of the scattering parameter, δ . In the upper panel, the figure indicates the maximum fluctuation in energy for each run. The amount of work required for each run is illustrated in the center and lower figures.

Figure 8 illustrates the difference in the computed trajectory of the fired atom for the controlled and uncontrolled method. By integrating the same problem with a very small stepsize, one can verify that the Adaptive Verlet solution is qualitatively correct. This particular problem has a strong three-body “collision”, which leads to a jump in energy during the numerical integration. The negative effects are reduced by the small timesteps taken by the adaptive method in the vicinity of the “collision”. The deviations from constant energy are shown in Figure 8. In this case, the g_2 control shows remarkable improvements in energy conservation, which lead to more accurate resolution of the dynamics. While one does not expect the integration of a scattering problem to produce exact trajectories, one would like the energy to remain approximately conserved. We have already shown that low-energy solutions (bounded trajectories) are qualitatively different those at higher energy levels. Approximate conservation of first integrals, such as energy, is a good indication that the qualitative behavior of the dynamics is correct.

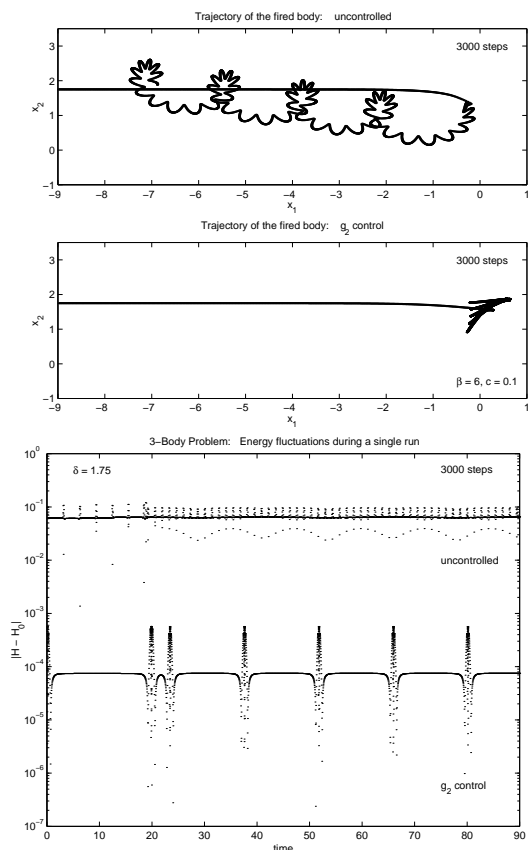


Figure 8. The improvements in the resolution of the dynamics of a 3-body scattering problem. The computed trajectories of the fired body for the controlled and uncontrolled methods, are shown in the upper and center panels. In the lower panel, the figure illustrates the improvements in energy conservation using the adaptive method.

5. Conclusions

Improvements of an order of magnitude or more, as seen here, are common in low-dimensional problems. There is a clear qualitative distinction between the symplectic and reversible methods which is already evident in this small example: the reversible scheme does not possess the “restraining hand” of a Hamiltonian perturbation expansion. Nonetheless, the long term stability of the method is similar to that of the symplectic integrator in long interval computations in low-dimensional applications.

For large systems the practical value of variable timesteps becomes less clear. This is a consequence of the typical ergodic behavior one expects which reduces the influence of time-localized events (e.g. caused by strong collisions). Another problem is that, in simulations of large systems, it seems that the loss of the nearby Hamiltonian expansion can sometimes lead to the possibility of systematic drift in the energy.

There are certain situations where adaptivity may prove highly desirable such as for chemical processes far from equilibrium where a change of state and dynamical behavior is observed over time. Other such problems may arise in

the conformational dynamics of proteins, e.g. where a sudden hinge motion may necessitate a smaller timestep. For such problems, the design of the stepsize control function g remains a challenging task.

References

- [1] G. BENETTIN AND A. GIORGILLI, *On the Hamiltonian interpolation of near to the identity symplectic mappings with application to symplectic integration algorithms*, J. Statist. Phys., 74 (1994), pp. 1117–1143.
- [2] E. HAIRER AND C. LUBICH, *The lifespan of backward error analysis for numerical integrators*, Numer. Math., 76 (1997), pp. 441–462.
- [3] S. REICH, *Backward error analysis for numerical integrators*, SIAM J. Numer. Anal., (submitted 1996).
- [4] J. M. SANZ-SERNA AND M. P. CALVO, *Numerical Hamiltonian Problems*, Chapman and Hall, New York, 1995.
- [5] J. WALDVOGEL, *A new regularization of the planar problem of three bodies*, Celestial Mechanics, 6 (1972), pp. 221–231.
- [6] K. ZARE AND V. SZEBEHELY, *Time transformations for the extended phase space*, Celestial Mechanics, 11 (1975), pp. 469–482.
- [7] E. HAIRER, *Variable time step integration with symplectic methods*, Applied Numerical Mathematics, 25 (1997), pp. 219–227.
- [8] W. HUANG AND B. LEIMKUHLE, *The Adaptive Verlet method*, SIAM J. Sci. Comput., 18 (1997), pp. 239–256.
- [9] P. HUT, J. MAKINO, AND S. MCMILLAN, *Building a better leapfrog*, The Astrophysical Journal, 443 (1995), pp. L93–L96.
- [10] B. LEIMKUHLE, *Reversible adaptive regularization: perturbed Kepler motion and classical atomic trajectories*, Phil. Trans. Roy. Soc., (submitted 1997). (NA Report, DAMTP, Cambridge).
- [11] D. STOFFER, *Variable steps for reversible methods*, Computing, 55 (1995), pp. 1–22.
- [12] U. M. ASCHER AND S. REICH, *On some difficulties in integrating highly oscillatory Hamiltonian systems*, Lecture Notes in Computational Science and Engineering, (to appear).
- [13] R. A. LABUDDE AND D. GREENSPAN, *Energy and momentum conserving methods of arbitrary order for the numerical integration of equations of motion. part I*, Numerische Mathematik, 25 (1976a), pp. 323–346.
- [14] ———, *Energy and momentum conserving methods of arbitrary order for the numerical integration of equations of motion. part II*, Numerische Mathematik, 26 (1976b), pp. 1–16.
- [15] J. C. SIMO AND O. GONZALEZ, *On the stability of symplectic and energy-momentum algorithms for nonlinear Hamiltonian systems with symmetry*, Comp. Meth. in Appl. Mech. Eng., 134 (1996), pp. 197–222.
- [16] Z. GE AND J. E. MARSDEN, *Lie-Poisson integrators and Lie-Poisson Hamiltonian-Jacobi theory*, Phys. Lett. A, 133 (1988), pp. 134–139.
- [17] E. BARTH, B. LEIMKUHLE, AND S. REICH, *A semi-explicit, variable-stepsize, time-reversible integrator for constrained dynamics*, SIAM J. Sci. Comput., (to appear).
- [18] S. CIRILLI, E. HAIRER, AND B. LEIMKUHLE, *Asymptotic error analysis of the Adaptive Verlet method*. preprint.
- [19] C. J. BUDD AND G. J. COLLINS, *Symmetry based numerical methods for partial differential equations*, in Proc. 1997 Dundee Conference on Numerical Analysis, Addison Wesley Longman, 1997, p. 16.
- [20] I. N. HERSTEIN, *Topics in Algebra*, John Wiley & Sons, New York, second ed., 1975.